JOURNAL OF THERMOPHYSICS AND HEAT TRANSFER
Vol. 15, No. 2, April–June 2001

Technical Notes

TECHNICAL NOTES are short manuscripts describing new developments or important results of a preliminary nature. These Notes cannot exceed six manuscript pages and three figures; a page of text may be substituted for a figure and vice versa. After informal review by the editors, they may be published within a few months of the date of receipt. Style requirements are the same as for regular contributions (see inside back cover).

Laser-Plasma Generator with Artificial Turbulence of the Input Gas Stream

Sergey T. Surzhikov*
Russian Academy of Sciences, 117526, Moscow, Russia

Nomenclature

c_p	=	specific heat at constant pressure
k	=	turbulent kinetic energy
L	=	length of a laser plasma generator chamber
N_g	=	number of spectral groups
P	=	laser radiation power
p	=	pressure
Q	=	heat-release capacity
R	=	radius
T	=	temperature
U	=	medium radiation density
u	=	x component of velocity
v	=	r component of velocity
x, r	=	cylindrical coordinates
$\Delta\Omega$	=	total spectral region
$\Delta\omega_g$	=	group spectral region
ε	=	dissipation rate of k
κ	=	absorption coefficient
λ	=	molecular conductivity
μ	=	molecular viscosity
ρ	=	density
χ_ω	=	absorption coefficient for the laser radiation caused by inverse of bremsstrahlung mechanism

Subscripts

b	=	radial boundary of nonfocused laser beam
bb	=	black body
c	=	caustic surface
eff	=	effective parameters
g	=	group quantities
HR	=	heat radiation
L	=	radial boundary of laser beam
LPG	=	boundary of a laser plasma generator chamber
t	=	turbulent parameters
w	=	surface
ω	=	spectral quantities

Introduction

A LASER plasma generator (LPG) represents one type of a laser plasma accelerator.[1] The geometry of the LPG is shown in Fig. 1. The LPG is represented as a cylindrical channel (labeled 2) in which at some distance x_1 from the entering section (labeled 4) a low-temperature laser plasma (labeled 3) is created as a result of absorption of focused laser radiation (labeled 1). Laser radiation flux (in this case with a CW CO_2-laser with a wavelength $\lambda = 10.6\ \mu$) is less than what is needed for optical gas breakdown, but sufficient for maintaining the plasma in the laser radiation field. The characteristic size of the laser plasma is determined by transverse size R_c of the laser beam in the place where this plasma is localized. Gas velocities at the entrance section of the LPG channel are low, about 1–20 m/s. The temperature inside the laser plasma ranges from 15,000–20,000 K, and the process takes place at almost constant pressure. Air at atmospheric pressure is considered in this study.

The numerical modeling of the thermal and gas dynamics structure of the LPG is carried out for the laser power 40–100 kW. Auto-oscillations of the gas flow are predicted as a result of the presence of high temperatures localized in space. By numerical experiments it is shown that artificial gas turbulence introduced at the entrance of the LPG-channel suppresses these auto-oscillations and increases the stability of laser plasma in the gas flow.

Presented as Paper 2000-2631 at the AIAA 31st Plasmadynamics and Laser Conference, Denver, CO, 19–22 June 2000; received 31 July 2000; revision received 28 September 2000; accepted for publication 28 September 2000.

*Professor, Head of the Computational Physical-Chemical and Radiative Gas Dynamics Laboratory, Institute for Problems in Mechanics, prospekt Vernadskogo 101; surg@ipmnet.ru.

Statement of the Problem and Governing Equations

To investigate the unsteady gas dynamic processes in the LPG, a radiative gas dynamic (RGD) computational fluid dynamic model is developed. This model is based on a system of equations of viscous heat-conducting gas dynamics, laser and selective radiative heat transfer. A peculiarity of the given model is the possibility to simulate nonstationary subsonic thermal and gas dynamic processes at any density difference and also taking into account the turbulent character of flows in the LPG channel. Real thermophysical and optical properties of high-temperature air are taken into account. The reader is referenced to previous work in developing the RGD models, specifically, Refs. 1 and 2.

The RGD model of the LPG in a two-dimensional cylindrical domain includes the following equations for conservation of mass and the momentum components and energy:

$$\frac{\partial\rho}{\partial t}+\frac{\partial(\rho u)}{\partial x}+\frac{1}{r}\frac{\partial(r\rho v)}{\partial r}=0 \tag{1}$$

$$\rho\left(\frac{\partial u}{\partial t}+u\frac{\partial u}{\partial x}+v\frac{\partial u}{\partial r}\right)=-\frac{\partial p}{\partial x}+\frac{4}{3}\frac{\partial}{\partial x}\left(\mu_{\text{eff}}\frac{\partial u}{\partial x}\right)+\frac{1}{r}\frac{\partial}{\partial r}\left(r\mu_{\text{eff}}\frac{\partial u}{\partial r}\right)+\frac{1}{r}\frac{\partial}{\partial r}\left(r\mu_{\text{eff}}\frac{\partial v}{\partial x}\right)-\frac{2}{3}\frac{1}{r}\frac{\partial}{\partial x}\left(\mu_{\text{eff}}\frac{\partial rv}{\partial r}\right) \tag{2}$$

$$\rho\left(\frac{\partial v}{\partial t}+u\frac{\partial v}{\partial x}+v\frac{\partial v}{\partial r}\right)=-\frac{\partial p}{\partial r}+\frac{\partial}{\partial x}\left(\mu_{\text{eff}}\frac{\partial u}{\partial r}\right)+\frac{\partial}{\partial x}\left(\mu_{\text{eff}}\frac{\partial v}{\partial x}\right)+\frac{4}{3}\frac{1}{r}\frac{\partial}{\partial r}\left(r\mu_{\text{eff}}\frac{\partial v}{\partial r}\right)-2\frac{\mu_{\text{eff}}v}{r^2}-\frac{2}{3}\frac{1}{r}\frac{\partial}{\partial r}\left(r\mu_{\text{eff}}\frac{\partial u}{\partial x}\right)-\frac{2}{3}\frac{1}{r}\frac{\partial\mu_{\text{eff}}v}{\partial r}+\frac{2}{3}\frac{\mu_{\text{eff}}}{r}\left(\frac{\partial u}{\partial x}+\frac{1}{2}\frac{\partial(rv)}{\partial r}\right) \tag{3}$$

$$\rho c_p\left(\frac{\partial T}{\partial t}+u\frac{\partial T}{\partial x}+v\frac{\partial T}{\partial r}\right)=\frac{\partial}{\partial x}\left(\lambda_{\text{eff}}\frac{\partial T}{\partial x}\right)+\frac{1}{r}\frac{\partial}{\partial r}\left(r\lambda_{\text{eff}}\frac{\partial T}{\partial r}\right)+Q_L-Q_{\text{HR}} \tag{4}$$

$$Q_L=\frac{\chi_\omega P}{\pi R_L^2}\exp\left(-\frac{r^2}{R_L^2}\right),\qquad \frac{\partial P}{\partial x}=-\chi_\omega(x,r=0)P \tag{5}$$

$$Q_{\text{HR}}=\int_{\Delta\Omega}\kappa_\omega(U_{\text{bb},\omega}-U_\omega)\,\mathrm{d}\omega=\sum_{g=1}^{N_g}\kappa_g(U_{\text{bb},g}-U_g)\Delta\omega_g \tag{6}$$

$$\frac{\partial}{\partial x}\left(\frac{1}{3\kappa_g}\frac{\partial U_g}{\partial x}\right)+\frac{1}{r}\frac{\partial}{\partial r}\left(\frac{r}{3\kappa_g}\frac{\partial U_g}{\partial r}\right)=-\kappa_g(U_{\text{bb},g}-U_g)\qquad g=1,2,\ldots,N_g \tag{7}$$

Here spectral group characteristics are introduced by averaging for each of the N_g spectral ranges $\Delta\omega_g$ in a total spectral region $\Delta\Omega$.

To calculate the heat-release capacity Q_L, a geometric optics approximation is used [see Eqs. (5)]. The focused laser beam radius R_L is modeled as $R_L = R_c + (x_1 - x)(R_b - R_c)/x_1$ at $x < x_1$; $R_L = R_c$ at $x_1 < x < x_2$; $R_L = R_c + (x - x_2)(R_b - R_c)/x_1$ at $x > x_2$.

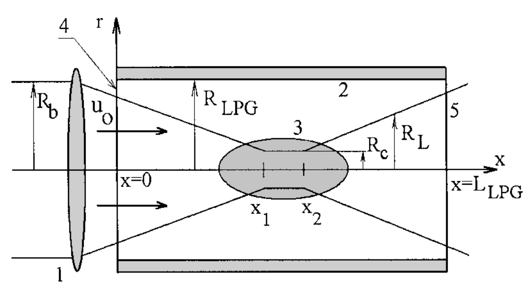

Fig. 1 Laser plasma generator schematic.

The equation of selective radiation transfer is integrated in the form of a multigroup P_1-approximation of the spherical harmonics method.[3] It is necessary to integrate a system of the N_g Eqs. (7) in order to calculate the heat-release capacity caused by radiation heat transfer Q_{HR}.

An internal cylindrical surface of the LPG channel ($r = R_{\text{LPG}}$; labeled as 2 in Fig. 1) is taken as absolutely black, and its temperature T_w is taken as constant equal to 300 K. The laser beam direction coincides with the x axis. At the input section of the channel ($x = 0$; labeled as 4 in Fig. 1), one specifies the axial velocity $u = u_0$ and the laser power $P(x = 0) = P_L$. At the exit section ($x = L_{\text{LPG}}$; labeled 5 in Fig. 1) the following boundary conditions are used: $x = L_{\text{LPG}}$, $\partial u/\partial x = \partial^2 v/\partial x^2 = \partial T/\partial x = \partial U_g/\partial x = 0$. The Gaussian distribution for the plasma temperature at $x = x_1$ with a maximum temperature of 18,000 K was assumed at an initial condition for the background of the undisturbed gas flow.

The process develops at approximately a constant pressure, which causes significant problems for a numerical solution of the problem, because the available disturbances for the pressure are hundreds of times less than the background pressure. However, in this case it is sufficient to take into account only the temperature dependencies of the thermophysical and optical properties (ρ, λ, μ, χ_ω, κ_g) using the local thermodynamic equilibrium approximation. The 18-group spectral model of a hot air in a spectral range $\Delta\Omega = 1{,}000$–$150{,}000\ \text{cm}^{-1}$ has been calculated with use of the computer system MSRT.[4]

Within the framework of the model, the process of turbulent mixing is taken into account using the Bousinesq hypothesis by introduction of the effective factor of turbulent viscosity μ_t, which is determined by one of the turbulence models. The mean effective viscosity is determined by using the formula $\mu_{\text{eff}} = \mu + \mu_t$, and the effective thermal conductivity is calculated through use of a turbulent Prandtl number $Pr_{\text{eff}} = \mu_{\text{eff}} c_p/\lambda_{\text{eff}}$, which is assumed to be unity.

The turbulent viscosity was modeled using the k-ε model of turbulence.[5] In this model the turbulent viscosity is determined by $\mu_t = C_\mu \rho k^2/\varepsilon$. The functions k and ε are calculated by the following set of equations:

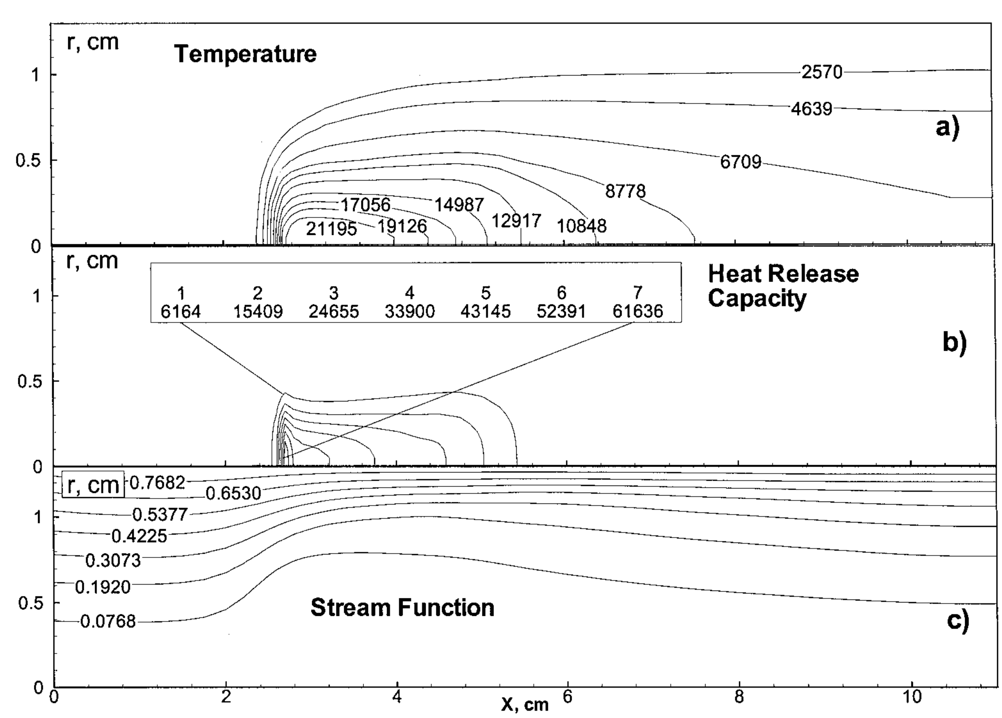

Fig. 2 Gas dynamic parameters of the LPG for $u_0 = 3$ m/s and $P_L = 40$ kW for laminar entrance flow: a) temperature contours (numbers near the curves are the temperature in K); b) heat release capacity caused by laser radiation Q_L, W/cm^3; and c) stream function.

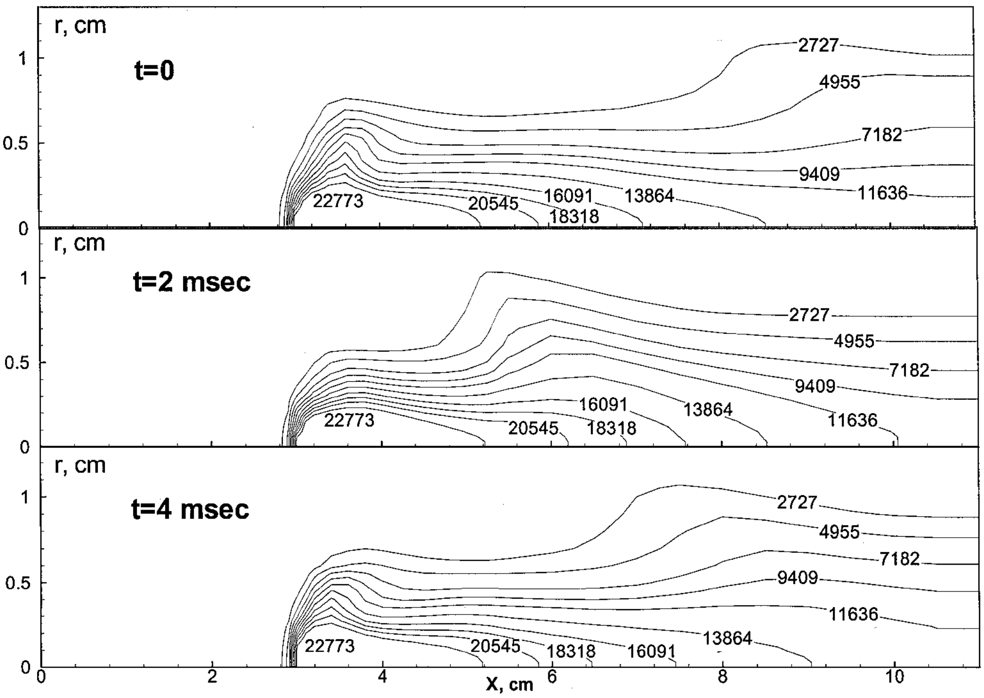

Fig. 3 Temperature contours for case $u_0 = 20$ m/s and $P_L = 100$ kW for laminar entrance flow at three sequential instants with a period 2 ms. Numbers near the curves are the temperature in K.

$$\frac{\partial \rho k}{\partial t} + \frac{1}{r}\frac{\partial}{\partial r}\left[r\left(\rho k v - \frac{\mu_t}{\sigma_k}\frac{\partial k}{\partial r}\right)\right] + \frac{\partial}{\partial x}\left(\rho k u - \frac{\mu_t}{\sigma_k}\frac{\partial k}{\partial x}\right) = S - \rho\varepsilon \tag{8}$$

$$\frac{\partial \rho \varepsilon}{\partial t} + \frac{1}{r}\frac{\partial}{\partial r}\left[r\left(\rho \varepsilon v - \frac{\mu_t}{\sigma_\varepsilon}\frac{\partial \varepsilon}{\partial r}\right)\right] + \frac{\partial}{\partial x}\left(\rho \varepsilon u - \frac{\mu_t}{\sigma_\varepsilon}\frac{\partial \varepsilon}{\partial x}\right) = (C_1 S - C_2\rho\varepsilon)\frac{\varepsilon}{k} \tag{9}$$

where

$$S = \mu_t\left\{2\left[\left(\frac{\partial v}{\partial r}\right)^2 + \left(\frac{\partial u}{\partial x}\right)^2 + \left(\frac{v}{r}\right)^2\right] + \left(\frac{\partial v}{\partial x} + \frac{\partial u}{\partial r}\right)^2\right\} - \frac{2}{3}\rho k\left(\frac{\partial u}{\partial x} + \frac{1}{r}\frac{\partial r v}{\partial r}\right) - \frac{\lambda_t}{\rho^2}\left(\frac{\partial \rho}{\partial r}\frac{\partial p}{\partial r} + \frac{\partial \rho}{\partial x}\frac{\partial p}{\partial x}\right)$$

$C_\mu = 0,09$; $C_1 = 1,44$; $C_2 = 1,92$; $\sigma_k = 1,0$; $\sigma_\varepsilon = 1,3$; $\lambda_t = c_p\mu_t$. The method of unsteady dynamic variables[6] was used to solve Eqs. (1–4). All finite difference equations are of second order in space (on an inhomogeneous grid, 81 × 81) by using the successive overrelaxation by lines method.

Numerical Simulations

To calculate the thermal and gas dynamic structure of the LPG, the following input data were set: $P_L = 40$–100 kW, $u_0 = 1$–20 m/s, $x_1 = 3$ cm, $x_2 = 3.5$ cm, $R_c = 0.21$ cm, $R_b = 0,5$ cm, $L_{\text{LPG}} = 11$ cm, and $R_{\text{LPG}} = 1.3$ cm.

The first series of the calculations was carried out for a laminar gas stream entering the LPG channel. The calculations began by assuming $u_0 = 1$ m/s. After achievement of a solution (which could be unsteady), the velocity was increased on 2 m/s, and the calculation was repeated. At specific velocity of the gas stream ($u_0 < 5$ m/s), the laser plasma moves toward the laser radiation, and its forward front terminates at a distance of approximately 2.5 cm from the channel entrance. In these cases the distributions of all thermal and gas dynamic functions were quickly stabilized and did not vary in time, that is, the steady-state solution was obtained.

Figure 2 shows the distributions for the thermal and gas dynamic functions in the steady-state case at $u_0 = 3$ m/s and $P_L = 40$ kW. Here the stream function is defined as

$$\psi = \int_0^r r\rho u \,\mathrm{d}r \Big/ \int_0^{R_{\text{LPG}}} r\rho u \,\mathrm{d}r$$

With increasing velocity u_0 the laser plasma is displaced closer to the geometric focal point (in this case at $x_1 = 3$ cm). At velocity u_0 of approximately 6–8 m/s, oscillations appear for the velocity and temperature. The amplitudes of these oscillations increase with u_0. Analogous phenomena are observed when increasing the laser power.

The temperature contours in the LPG channel at $u_0 = 20$ m/s and $P_L = 100$ kW in sequential instants of 2 ms are shown in Fig. 3. Separate phases of the self-oscillating process are clearly visible. Acoustic perturbations of pressure, large-scale perturbations of density and velocity vary with time in accordance with the temperature changes.

From the point of view of fundamental gas dynamics, the process of auto-oscillations of a stream behind a localized area of energy release is interesting and is worth further study. But from an applied point of view, the origin of auto-oscillations is an undesirable phenomenon because these can promote the cancellation of the laser-supported plasma.

Studies that explain the possibility to suppress these auto-oscillations of a gas stream are planned using the model presented here. It is assumed that in an entering section of the channel it may be possible to create artificial turbulence in the gas stream. It was established by the numerical calculations that suppression of large-scale stream auto-oscillations can be reached at high (but realizable in practice) 20% oscillation amplitude of the entrance flow velocity. Steady-state distributions for the thermal and gas dynamic functions obtained for 20% turbulence of the entrance flow are shown in Fig. 4. In this case the initial turbulence of the stream was simulated by the setting $k = 0.1$ and $\varepsilon = 0.1$ at the entering section ($x = 0$). At a smaller level of initial turbulence, the suppression of

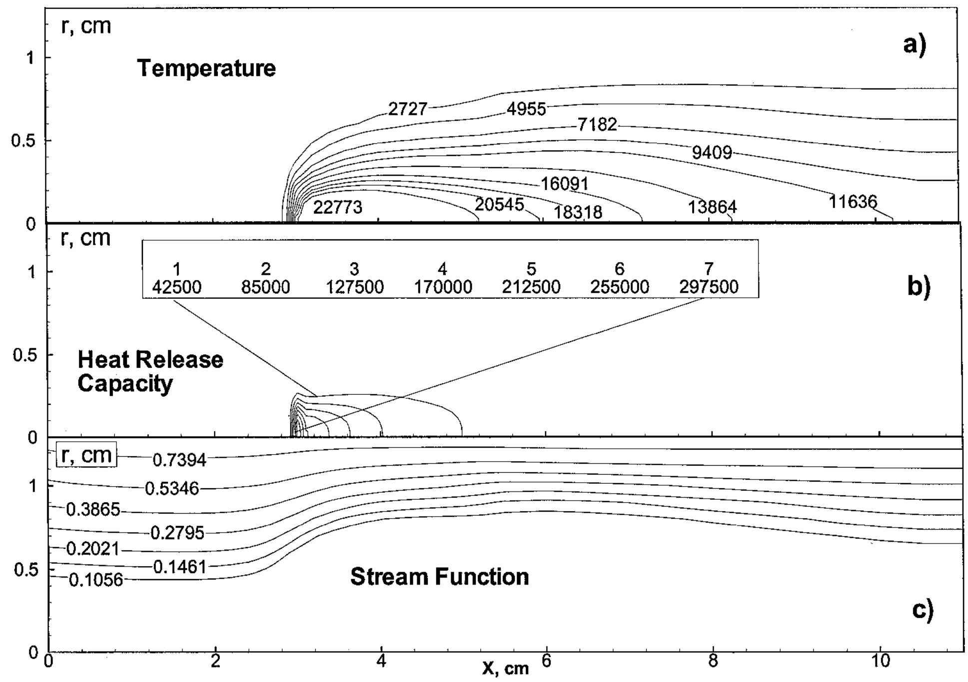

Fig. 4 LPG gas dynamic parameters for $u_0 = 20$ m/s and $P_L = 100$ kW with turbulence entrance flow: a) temperature contours (numbers near the curves are the temperature in K), b) heat release capacity caused by laser radiation Q_L, W/cm^3, and c) stream function. Steady-state solution.

auto-oscillations of the stream is less. For example, at $k = 0.01$ the influence of initial turbulence on thermal and gas dynamic functions is negligible.

Conclusions

An unsteady radiative gas dynamic numerical simulation model of a laser plasma generator with turbulent gas stream is presented. This model is based on a system of coupled Navier–Stokes equations, laser radiation transfer and selective radiation heat-transfer equations, and also equations for the k-ε model of turbulence.

It is determined that auto-oscillations of gas stream in the LPG do appear at certain critical input parameters. It was shown that a practical way to stabilize the gas dynamic structure in a LPG is by artificial turbulence of the input gas flow. The intrinsic gas-flow auto-oscillations in the LPG chamber may be suppressed by generation of as little as 10–20% amplitude oscillation for the input gas velocity.

Acknowledgments

This work has been supported by Russian Foundation of Basic Research (Project N 98-02-17728). The support and discussions with Professor H. Krier are greatly appreciated.

References

[1]Glumb, R. J., and Krier, H., "Concepts and Status of Laser-Supported Rocket Propulsion," *Journal of Spacecraft and Rockets*, Vol. 21, No. 1, 1984, pp. 70–79.

[2]Conrad, R., Raizer, Yu. P., and Surzhikov, S. T., "Continuous Optical Discharge Stabilized by Gas Flow in Weakly Focused Laser Beam," *AIAA Journal*, Vol. 34, No. 8, 1996, pp. 1584–1588.

[3]Kourganoff, V., *Basic Methods in Transfer Problems*, Dover, New York, 1963, pp. 90–101.

[4]Surzhikov, S. T., "Computing System for Mathematical Simulation of Selective Radiation Transfer," AIAA Paper 2000-2369, June 2000.

[5]Jones, W. P., and Launder, B. E., "The Calculation of Low-Reynolds-Number Phenomena with a Two-Equation Model of Turbulence," *International Journal of Heat and Mass Transfer*, Vol. 16, No. 6, 1973, pp. 1119–1130.

[6]Surzhikov, S. T., "Numerical Simulation Method for Slow Unsteady Flows Near to Local Heat Release Regions," AIAA Paper 98-2829, June 1998.

Statistical Heat Transfer from Uniform Annular Fins with High Thermal Conductivity Coating

Antonio Campo*
Idaho State University, Pocatello, Idaho 83209

Nomenclature

Bi	=	Biot number, ht/k
c	=	inner-to-outer radii ratio, r_1/r_2
h	=	convection coefficient, W/m^2 · K
$I_\nu(\cdot)$	=	modified Bessel function of first kind and order ν
$K_\nu(\cdot)$	=	modified Bessel function of second kind and order ν
k_1	=	thermal conductivity of material 1, W/m · K
k_2	=	thermal conductivity of material 2, W/m · K
$\bar{k}$	=	generic spatial mean of the thermal conductivities k_1 and k_2, W/m · K
L	=	length, $r_2 - r_1$, m
L_t	=	total length, $r_2 - r_1 + t_2$, m
Q	=	heat transfer rate, W
Q_i	=	ideal heat transfer rate, W
R	=	normalized dimensionless r, r/r_2
r	=	radial variable, m
r_1	=	inner radius, m
r_2	=	outer radius, m
T	=	temperature, K
T_b	=	base temperature, K
T_∞	=	fluid temperature, K
t	=	total semithickness, $t_1 + t_2$, m

Received 10 April 2000; revision received 25 September 2000; accepted for publication 27 October 2000.

*Professor, College of Engineering. Member AIAA.